

High efficiency industrial type PERC Solar Cell on very thin EFG Substrates

P. Choulat¹, Y. Ma¹, BT. Chan¹, J. John¹, H. Nagel², J. Horzel², S. Forment³, G. Agostinelli^{1,4}, G. Beaucarne¹

¹IMEC vzw, Kapeldreef 75, B-3001 Leuven, Belgium

²SCHOTT Solar GmbH, Carl-Zeiss-Str. 4, 63755 Alzenau, Germany

³KaHo Sint-Lieven, Gebroeders Desmetstraat 1, 9000 Gent, Belgium

⁴Now with Good Energies, Zug, Switzerland

Tel: +32 16 28 83 11 Fax: +32 16 28 15 01 e-mail: Patrick.Choulat@imec.be

ABSTRACT: In this paper, we report on high efficiency industrial type solar cells on very thin EFG substrates of 100 μm^2 : 15.6% on 140 μm thick, and 16% on 170 μm thick on a base resistivity of 3 Ohm cm and 1 Ohm cm respectively. In both solar cells structures, we adopt a well passivated rear surface and local contacts. The process used in this work combines the advantage of using the applicability of a low quality oxide associated with a PECVD Silicon Nitride for the rear passivation and the use of the existing industrial technique for screen printing and contacts co-firing. In addition, to reduce front reflectance and enhance optical confinement, plasma technology using SF_6/Cl_2 chemistry is chosen to develop a well suited texturing process for shiny EFG surfaces. A Voc of 624 mV was achieved on the 1 Ohm cm EFG substrate, and a gain of about 1% in absolute efficiency compared to the classical Al BSF cell concept is observed. We show that an absolute gain of 0.85 mA/cm^2 is attained by means of front texturing only, and that an additional gain of 0.4 mA/cm^2 is obtained by reducing rear surface recombination velocity and by increasing internal rear reflectance when replacing the Aluminium contact by a dielectric stack.

Keywords: Light trapping, Plasma texturing, Solar Cell Efficiencies, Ribbon Si

1 INTRODUCTION

The trend to reduce the share of expensive high purity Silicon in solar cells and modules stems from the necessity to enable PV energy to become cost-effective. The use of thinner multi-crystalline substrates of course is a way to reduce material cost. Yet, this is somehow limited by the kerf loss which represents nowadays about 40% of the Si consumption from the brick to the wafer. This ratio is bound to become larger and larger as the wafer thickness reduces, limiting to some extent the positive effect of wafer thinning. An alternative to produce bulk silicon substrates is the EFG technology (Edge defined Film-fed Growth)[1]. EFG silicon is produced by Wacker SCHOTT Solar. The main advantage of using EFG substrates is that it totally eliminates the kerf loss associated with mechanical sawing. However, like most low-cost multicrystalline silicon materials, EFG silicon contains impurities (carbon in high concentration) and high concentrations of crystalline defects, which degrade the as-grown minority carrier lifetime to less than 10 μs . With a laboratory process including extensive material enhancement steps, efficiencies above 18 % have been demonstrated [2]. Efficiencies above 15% on large-area EFG substrates with a thickness below 200 μm have already been reported with the current industrial technology [3]. Nevertheless, to further improve solar cells performance, it was our interest to investigate advanced solar cell structures applied to EFG substrates.

The main bottlenecks are the presence of the full plane of Al on the rear which provides a moderate rear passivation, and the absence of surface texturing which, to a great extent, limits the possibility to reach high currents. Calculations (PC1D) show that if we assume a substrate of 140 μm with a bulk diffusion length of 300 μm (the minority carrier lifetime increases drastically

after all processing steps during the solar cell fabrication of EFG substrates [4]), reducing the rear surface recombination velocity from 1500 cm/s to only 800 cm/s [8] with a dielectric and increasing internal rear reflectance from 60% with screen printing Al to 90% with a dielectric stack, would lead to an efficiency increase of 0.7%. Moreover, by applying front surface texturing, further improvements can be attained.

Essential in this passivated rear structure which replaces the full plane of Aluminium on the rear by a dielectric stack of SiO_2 and SiN , is the nature of the rear oxide which is of lower quality than a thermal oxide but nonetheless provides low rear surface recombination velocities [5,8]. High temperatures as well as long processing time are therefore not required and make the process industrially compatible for such EFG substrates.

2 EXPERIMENTAL

2.1 Solar cells

We processed a batch of selected material, 100 cm^2 EFG substrates of 1 Ohm cm and 3 Ohm cm with a starting thickness before processing of 170 μm and 140 μm respectively. Part of the batch was passivated with a dielectric stack of deposited SiO_2 and PECVD SiN while the rest, for fair comparison, had a rear structure with a full Al BSF. The process sequence comprises for both groups, a front plasma texturing structure, an identical emitter of 72-75 Ohm/sq in conjunction with a low PECVD SiN for antireflection coating (ARC), and screen printed Ag contacts. In the *i*-PERC cells, the passivation stack was locally opened in a dot array pattern with a Nd:YAG laser to enable local contacts of Al. The structure combined with the contact firing, ensures the presence of a local BSF in those areas.

2.2 Front surface texturing

As grown EFG substrates have a polished surface on a microscopic level. To adapt a front surface texturing step, suitable for such substrates, we first carried out preliminary tests. We subjected CZ substrates under different chemistry of plasma etching to determine what process recipe to use. The wafers were chemically prepared and etched to have an identical front shiny surface as the EFG wafers before plasma texturing. The wafers were then processed to final solar cells, having a classical rear Al BSF for analysis and comparison. The results will be discussed later.

2.3 Extraction of internal reflectance

CZ-Si substrates were prepared with an identical structure as the final solar cells for reflectance analysis. All substrates were coated with a front SiN ARC. On the rear, two different structures were formed: a screen-printed Al and a dielectric stack/screen-printed Al, for the full Al BSF and the *i*-PERC cell structure respectively. To reproduce the refractive index of the deposited layers in a finished solar cell, the wafers were subsequently fired in a conveyor belt furnace. To avoid erroneous interpretation and to ensure we could exploit the near infrared region of the spectrum from standard hemispherical measurements, the substrates were initially chemically thinned to 90 microns and were devoid of emitter and of front Ag contacts. The reflectance curves of these test structures were then measured and analysed.

3 FRONT SURFACE TEXTURING

One of the main challenges was to find a suitable front surface texturing for such substrates which present a shiny surface as grown. Alkaline texturing which works well on a specific crystallographic orientation of (100) grains could be applied on EFG ribbons, but the surface would result in an anisotropic texturing as they exhibit various longitudinal grains of different orientations. Texturing EFG Si wafers by mechanical grooving does not seem to be an appropriate candidate for industrial processing either. The wavy nature of EFG Si substrates would require to groove very deep into the wafer. In some cases the waviness of the wafers is as high that it would not be possible to groove the complete wafer surface without cutting through the wafers. Thus, the mechanical yield of such a process would be too low to be of interest for industrial production scenarios. However, one elegant solution is to use plasma technology. We use a reactor based on microwave dissociation of a gas mixture containing SF₆, N₂O and Cl₂. The method combines the advantage of creating an isotropic surface texturing for low reflectivity and reduces the Si consumption to a few microns only. The technique is all the more attractive as it can be applied on all kind of surface topography. Extensive studies have been dedicated on this topic and etching mechanism has also been reported in the last 4 years [9,11].

Nevertheless, despite the fact that no initial surface roughness is required, the process parameters still have to be adapted to reach good uniformity for different type of surfaces. Indeed, due to the configuration of our reactor, which has 2 parallel antennas above the substrates, the formation of the texturing does not happen equally across

the surface. Areas located far away from the MW antennas have a slower texture formation than those underneath the antennas. As a consequence, we experimentally observed that a process recipe well adapted for as-cut multicrystalline Si substrates does not give the same results on shiny surfaces because large areas on the EFG substrates were left completely untextured. To reach a good uniformity we prolonged the etching using the same halogen gas composition but the surface appears to be rather dark (condition A). Closer inspection with scanning electron microscope (SEM) reveals high roughness at microscopic level (Figure 1). This morphology is likely to be detrimental for the solar cell performance. Therefore, a new process recipe specific to shiny EFG surfaces with different gas ratio as well as different partial pressures was developed to reach to the same performance as for the as-cut multicrystalline Si substrates recipe and to obtain a good uniformity across the silicon surface area (condition B shown in Figure 2).

To illustrate the above observation, a batch of CZ substrates was processed as explained in section 2.2. The results are compared in Figure 3. We also introduced a group of acidic isotextured wafers, taken as a reference and a group of polished wafers (similar surface as for EFG substrates). One can see in Figure 1 that despite the low reflectivity for condition A (14% at 700 nm), the surface morphology is too rough and therefore creates a damage layer favourable to recombination, resulting in lower J_{sc} and lower V_{oc} shown in Figure 3. By changing the SF₆/N₂O ratio, which modifies the balance between etching and redeposition of the etching products, and by adapting the Cl₂ step which flattens the textured structure for condition B, a more defined topography is created on the surface (Figure 2). This results in an increase in reflectivity (21% at 700 nm) but nevertheless recovers V_{oc} as well as J_{sc} due to the elimination of the surface damage.

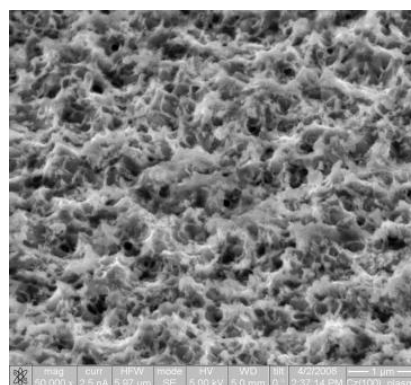


Figure 1: Texturing surface using condition A. Low reflectivity (14% @ 700 nm) but unsuitable for solar cell

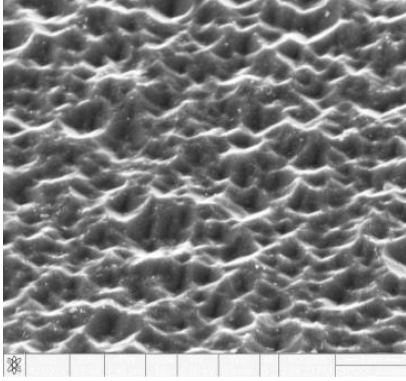


Figure 2: Texturing surface using condition B. Conditions adapted for polished EFG surfaces. High reflectivity (21% @ 700 nm) but no surface damage

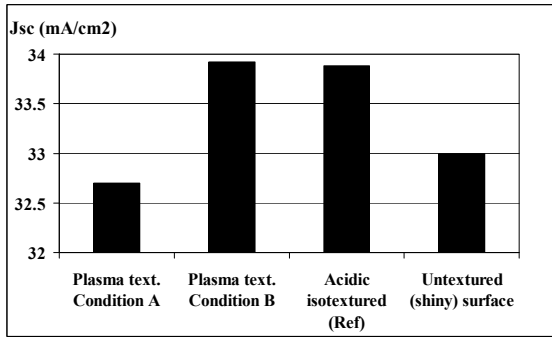


Figure 3: Short circuit current trend on CZ Si substrates (1 Ohm.cm, 250 μm thick), having different front surface topography. Condition B is chosen for the EFG substrates

Furthermore, one can see the substantial gain potential of the short circuit current between the untextured and plasma textured surface. A net gain of 0.9 mA/cm² is observed at cell level (4 cells per group). The comparison was also carried out on 200 μm thick mc-Si substrates and the same difference in J_{sc} was measured. Following these results, we calculated using PC1D, the gain potential of the short circuit current. The input parameters into the model were identical for both structures as far as the rear and the bulk of the substrates were concerned (emitter characteristics, wafer thickness, bulk lifetime and rear surface passivation). The parameters which differed for both cell designs were the front reflectivity and the internal rear reflectance since light trapping differs due to the different front surfaces. Reflectance curves were measured from 300 nm to 1200 nm as explained in section 2.3 and introduced in the PC1D model. The internal rear reflectance was calculated from an optical model, set out in section 4. The calculations show, considering the type of substrates under study, that a gain of about 1 mA/cm² in absolute value is achievable. This result is in good agreement with what we observed experimentally. In terms of efficiency, suitable front texturing to the EFG substrates leads to an improvement of 0.4% absolute compared to polished surfaces.

4 LIGHT TRAPPING

The introduction of the PERC cell concept is obviously primarily used to reduce the rear surface

recombination velocity in comparison with a classical Al BSF rear structure, which leads to higher open circuit voltage and also to higher short circuit current (J_{sc}). Nevertheless, the main gain in J_{sc} is generated when introducing an excellent back reflector. The addition of an oxide at the Si interface makes the Si/SiO₂/SiN/Al makes the architecture highly favourable in the *i*-PERC design for better light trapping. We therefore carried out reflectivity measurements on the 3 different following structures as explained in section 2.3:

- Untextured (flat) front surface with full Al BSF on the rear (current industrial structure for EFG).
- Plasma textured (Condition B) front surface with full Al BSF on the rear.
- Plasma textured (Condition B) front surface with the Si/SiO₂/SiN/Al structure and local contacts on the rear.

Using the reflectivity curves (Figure 4), we extracted using the model shown below, the internal reflectance (R_B) to quantify how much current we could gain when one improves the light trapping in the substrate.

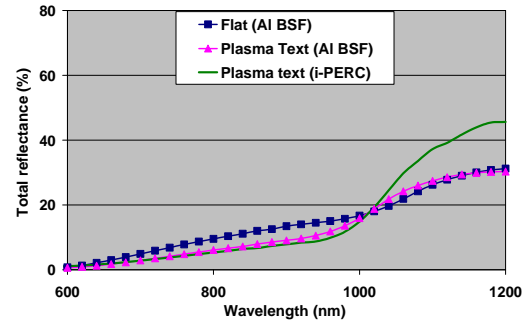


Figure 4: Total reflectance (R_{total}) as a function of wavelength. Measurements done with a standard set up, with integrating sphere.

The total reflectance is defined to be the sum of the front reflectance (R_{Front}) and the escape reflectance (R_E). R_E, in turns, depends on the internal front reflectance (R_F) and on R_B (Figure 5).

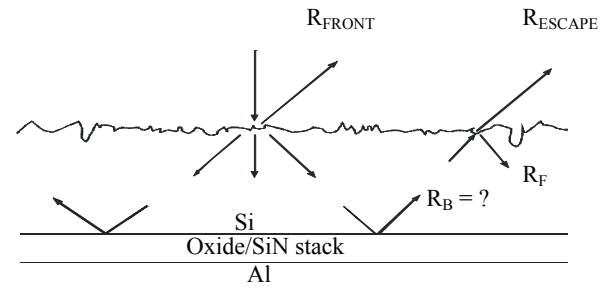


Figure 5: Optical model of the cell structure

It can be shown that, R_{Total} can be written as follow:

$$R_{Total} = R_{Front} + \frac{R_B(1 - R_F)(1 - R_{Front})e^{-2\alpha W}}{1 - R_B R_F e^{-2\alpha W}}$$

With

- $m = 1/\cos\theta$, θ being the angle of the rays to the normal.
- α = Absorption coefficient of Si.
- W = Wafer thickness.

For randomised light (case b and c), the internal front reflectance can also be expressed as:

$$R_F = 1 - \frac{1 - R_{Front}}{n_{Si}^2} \quad (1)$$

With n_{Si} = Refractive index of Silicon.

For a flat front surface (case a), the internal front reflectance can be expressed as:

$$R_F = R_{Front} \quad (2)$$

More information about this method can be found in [12]. In the case of the untextured surface, the extracted value of R_B in the long wavelength was found to be abnormally low ($< 10\%$) and therefore unrealistic. Indeed, internal reflectance of Si-Al interface was also calculated using SUNRAYS. For all angle of incidences ranging from 0° to 90° , reflectance between 1100 nm and 1200 nm varies only by 2 % only, which contradicts our extracted values of R_B because in the case of plasma textured front surface with identical rear, R_B is found to be 68%. The model assumes a flat front surface and a perfectly flat interface between Si and Al to validate the expression of R_F in (2). However, further analysis showed that the interface in the fabricated cell structures is far from being flat. Indeed, for the formation of the Al BSF, we use a screen printed Aluminium paste which consists of Aluminium particles, a glass frit, organics binders and solvents. After firing the cell to create the BSF, the resulted interface becomes rough enough to change the reflected light in many directions. As a consequence, after the first incoming path, the light is probably randomised on the rear which changes the configuration of our model. We therefore consider the rear surface as being 'semi' Lambertian, and we make the assumption that the expression of R_F is closer to equation (1). R_B was recalculated in the long wavelength and the results are summarised in table 1.

	Flat AlBSF	Textured AlBSF	<i>i</i> -PERC
Internal reflectance, R_B	62%	67%	91%

Table 1: R_B calculated from 1100 nm to 1200 nm.

One can see in Table 1 that the value of R_B for the untextured structure is clearly more realistic. Yet, the difference of 4% in internal reflectance between the flat and textured cell, is higher than expected when using SUNRAYS to calculate R_B for various angle of incidence. The above values were used in section 3 to calculate the gain potential of the short circuit current between untextured and plasma textured surfaces. Besides, one can see that the Oxide stack/Al system offers an excellent back reflector with a value of 91%, including the contribution of the metal point contacts. This result is in excellent agreement with values obtained during previous studies [8]. Moreover, the calculations

showed that the values of R_B remain constant over the range of wavelength under study.

5. CELL RESULTS

As explained in section 2, we processed a batch of selected material, 100 cm² EFG substrates with different bulk resistivity of 1 Ohm cm and 3 Ohm cm and with a starting thickness before processing of 170 μ m and 140 μ m thick respectively. The results of the best *i*-PERC solar cell are shown in Table 2 and Table 3, along with those of the best Al-BSF cell:

170 μ m 1 Ohm.cm EFG	Jsc [mA/cm ²]	Voc [mV]	FF [%]	η [%]
<i>i</i> -PERC	33.57	624	76.28	16
Al BSF Textured	33.11	606	77.73	15.6
Al BSF Untextured	32.23	608	77.39	15.15

Table 2: Best 100 cm² EFG cells on 1 Ohm cm p-type material, 72-75 Ohm/sq emitter. The cells are tabbed.

140 μ m 3 Ohm.cm EFG	Jsc [mA/cm ²]	Voc [mV]	FF [%]	η [%]
<i>i</i> -PERC	33.76	602	76.72	15.6
Al BSF Textured	32.6	582	77	14.6

Table 3: Best 100 cm² EFG cells on 3 Ohm cm p-type material, 72-75 Ohm/sq emitter. The cells are tabbed.

In this batch, all cells were processed with a 72-75 Ohm/sq diffused POCl₃ emitter associated with a standard Ag screen printed technology. For both bulk resistivities, the efficiencies of all the *i*-PERC cells are well above the efficiencies of the full Al BSF cells. Furthermore, the best Al BSF cell and the worst *i*-PERC cell show a difference of Voc of 10 mV. Even though it is very difficult to make a fair comparison due to the unique grain structure and therefore quality of each EFG wafer, we evaluated with PC1D that the rear surface recombination velocity is reduced by a factor of 3 when replacing the Al by a dielectric on the rear. Furthermore, the J_{sc} gain is confirmed when only applying a suitable plasma texturing process for such shiny surfaces. The average current gain observed of 0.85 mA/cm² (4 cells per group) is slightly lower than predicted in PC1D but is nevertheless substantial.

The best efficiency was 16 %, obtained on a 170 μ m thick EFG ribbon. This is not as high as the best solar cell reported in [3], but this refers to thinner ribbons without second ARC. Importantly, the techniques developed for the excellent results in [3] are complementary to those developed for the present results. In particular, the dielectric passivation here clearly enables a higher Voc and is beneficial for light confinement. Combining this with an emitter diffusion optimised for EFG and with a more adapted front side contacting, efficiencies approaching 17 % on very thin EFG ribbons are within reach.

6. CONCLUSION

In this work, we have reported high efficiency industrial type solar cells fabricated from thin EFG Si substrates. We demonstrated that the current limitation of EFG substrates due to the difficulty of texturing such polished surfaces can be overcome by using an adapted plasma texturing process. Experimentally, a net gain of nearly 0.9 mA/cm^2 is reached when reducing the average front reflectance. In addition to this technological step, further improvement was obtained by replacing the Al on the rear by a dielectric stack. Optical measurements and analysis showed an internal reflectance above 90% with the *i*-PERC cell concept. This results in further improvement of the short circuit current. Moreover, the integration of this dielectric stack reduces the rear surface recombination velocity to a great extent and gives rise to a significant increase in Voc. Finally, the advantage of integrating such a low quality oxide dielectric is all the more attractive as it eliminates the industrial constraints of long processing time as well as high temperatures which renders the process industrially compatible with EFG substrates.

ACKNOWLEDGEMENTS

This work was partially funded by the European Commission under the FP6 project CRYSTAL CLEAR, contract SES6-CT-2003-502583.

6. REFERENCES

- [1] W. Schmidt, B. Woesten, J. P. Kalejs, Prog. Phot. Res. Appl (2002), vol. 10, p. 129-140.
- [2] M. Kaes, G. Hahn, A. Metz, G. Agostinelli, Y. Ma, J. Junge, A. Zuschlag, D. Groetschel, Proceedings 22nd European Photovoltaic Solar Energy Conference (2007) 897-902.
- [3] J. Horzel, A. Seidl, W. Schmidt, Proceedings 20th European Photovoltaic Solar Energy Conference (2005, Barcelona) p. 698-701.
- [4] J. Horzel, A. Seidl, T. Grahl, 21st EU PVSEC (2006, Dresden), p. 655,660
- [5] G. Agostinelli, P. Choulat, H. Dekkers, 20th EU PVSEC (2005), Barcelona, Spain
- [6] G. Agostinelli, P. Choulat, H. Dekkers, 4th IEEE World Conference on Photovoltaic Energy Conversion (2006), Waikoloa, Hawaii
- [7] G. Agostinelli, P. Choulat, Y. Ma, 21st EU PVSEC (2006), Dresden, Germany
- [8] P. Choulat, G. Agostinelli, Y. Ma, F. Duerinckx, 22nd EU PVSEC (2007), Milano, Italy
- [9] H.F.W. Dekkers, G. Agostinelli, 19th EPVSEC, (2004), Paris
- [10] H.F.W. Dekkers, F. Duerinckx, L. Carnel, 21st EU PVSEC (2006), Dresden, Germany
- [11] H.F.W. Dekkers, “ *Study and optimisation of dry process technologies for thin crystalline silicon solar cell manufacturing*”, PhD thesis, KUL, May 2008
- [12] F. Duerinckx et al, Progress in Photovoltaics, (2005), vol 13, p 673-690